Journal of Physical and Theoretical Chemistry
of Islamic Azad University of Iran, 16 (3, 4) 103-116: Fall 2019 & Winter 2020
(J. Phys. Theor. Chem. IAU Iran)
ISSN 1735-2126

Theoretical Approach for Detection of $POCl_3$ Molecule by the Boron Nitride Nanosheet-based Sensing Nanodevices

Roghayeh Moladoust *

Department of Chemistry, Faculty of Basic Sciences, University of Mohaghegh Ardabili, Ardabil, Iran

Received January 2020; Accepted February 2020

ABSTRACT

To detect $POCl_3$ molecule, adsorption phenomena of this molecule on the pure, Al- and Si-doped BN sheet surfaces were investigated via density functional theory (DFT) approach. The most stable adsorption complexes, including $POCl_3$/BN (O-B), $POCl_3$/Al-BN (O-Al), and $POCl_3$/Si-BN (O-Si), were predicted with the adsorption energies of about -8.64, -37.01 and, -62.01 kcal mol^{-1}, respectively. Upon the adsorption process, the computational parameters indicated that the interaction of $POCl_3$ with Si-BN sheet was highly strong energetically, rationalizing more reactivity of the Si-BN to $POCl_3$, which led to the dissociation of this toxic molecule into the lower toxicity fragments with less harm to environmental protection. However, very strong interactions are not propitious in the sensing performance because of the high recovery time of the sensor. Based on the density of states (DOS) analysis, it was also revealed that the electronic sensitivity of the Al-BN sheet to $POCl_3$ increased with a significant variation by about -27.99% in the HOMO/LUMO energy gap. These changes are confirmed by the large electron charge transfer (Q_T) from $POCl_3$ molecule to the sheet surface and appearance the electronic new states within the energy gap (E_g). As a result, the changes in the electronic conductivity of the sheet create an electrical signal in the electronic circuit for detecting $POCl_3$ in the surrounding. Therefore, Al-BN possesses a more efficient function as a potential resource in the gas sensors.

Keywords: BN nanosheet; Density functional theory; Phosphoryl chloride; Sensing properties

1. INTRODUCTION

Phosphoryl chloride ($POCl_3$) is a hazardous molecule for human health. It is likely highly toxic by immersing, lethal by breathing, and noxious through skin absorption, creating vigorous burns and leading to scarring. Its application in the laboratory, including a drying agent and intermediate for the production of various kinds of materials, can be used to manufacture mixtures in the medical industry. It can also be used to produce chemical weapons of nerve gas [1]. Hence,

*Corresponding author: moladoust_100@yahoo.com

designing and fabrication of extremely sensitive, credible, rapidly reactive, selective, portable, and valid inexpensive sensors for detection of this toxic molecule are the challenging issues in the sensing fields. So far, various nanostructures containing nanotubes and nanosheets have been explored due to the high surface to volume ratios and greater electronic sensitivity. These features enable them to enhance the adsorption capacity and raise gas sensor character [2-8]. Numerous nanostructure-based sensors have been already expanded for various gases based on experimental and theoretical methods [9-13]. Since experimental techniques require expensive tools and are not sufficiently sensitive, a few theoretical approaches have been created to determine sensing properties of nanomaterials toward chemicals [14-18]. One of the simplest methods is based on variations in HOMO/LUMO energy gap (E_g) of the sensor upon the adsorption process through DFT computations [19-21]. Several investigations have been performed on the BN nanostructures because of their remarkable properties such as high thermal conductivity, chemical stability, wide band gap, strong resistance to oxidation, less toxicity, and chemical inertness [22-25]. The graphene-like BN nanosheet is one of the nanostructure species that possesses a stronger B-N bonding, with higher thermal and chemical stability of BN nanosheet than that of graphene, leading to improvement of the thermal and mechanical properties. Therefore, these structures have extensive applications in insulators, skincare products, solid lubricants, pencil leads, and so on [26, 27]. Also, further efforts have been made to improve the sensing function of the nanostructures. For instance, it has been shown that the inclusion of various impurities, as well as the creation of structural defects into the surface of nanostructures, cause changes in their electronic properties. Zhang et al. studied the adsorption of CO molecule on Al-doped, mono-vacancy and stone-wales defected h-BN and reported that the modified sheet was more sensitive to detect CO molecule than the pristine one [28]. Liu et al. found that the interaction of Fe@BNNT with NO_2 molecules was energetically more favorable than that of the pristine and 0.38 e charge transfer (Q_T) between them, indicating the enhancement of electrical conductance of the structure [29]. Zhang et al. showed that the HCOH molecule could be chemisorbed (strong interaction) to Si-BNNTs [30]. Synthesis of Si-doped BN nanotubes has recently been reported through chemical vapor deposition. Theoretical computations indicated that substituting a B atom of BNNTs by a Si atom resulted in the sizable narrowing of gap energy of BNNTs [31]. For the first time, the current letter reports the adsorption effects of $POCl_3$ molecule on the electronic properties changes of the bare BN nanosheet and its impurities within DFT formalism. This study aimed to discover the nanosheet potential features for detecting and monitoring toxic gases in residential and industrial environments.

2. THEORETICAL METHOD

The structural and electrical properties of BN-nanosheet and its derivatives were evaluated here to determine the sensor capability for detecting gas molecules. To this end, the adsorption process of $POCl_3$ molecule on the sheets surfaces was investigated with M06-2X density functional and 6-31+G(d) basis set as executed in the Gaussian 09 electronic structure package [32]. A previous report indicates that M06-2X density functional delivers reasonable results for adsorption energies, thermochemical features, and non-covalent interactions [33]. Initially, all available configurations were optimized in

the same level of computation as mentioned above. The values of adsorption energies were computed matching with the following formula:

$E_{ad} = E_{tot}$ ($POCl_3$/BN) – E_{tot} (BN) – E_{tot} ($POCl_3$) + E (BSSE) (1)

in which E_{tot} ($POCl_3$/BN), E_{tot} (BN), and E_{tot} ($POCl_3$) are the total energy of $POCl_3$-BN complex, isolated (BN, Al-BN and Si-BN) sheet, and single $POCl_3$ molecule, respectively. E (BSSE) is the basis set superposition error (BSSE) obtained by the Boys–Bernardi counterpoise method [34]. Frontier molecular orbital (FMO) and molecular electrostatic potential (MEP) surface analyses and all energy computations were carried out by the same M06-2X/6-31+G(d) level of theory. To measure the electronic sensitivity, the changes of HOMO/LUMO gap (E_g) as a proper index is determined by:

$\Delta E_g = [(E_{g2} – E_{g1})/E_{g1}]*100$ (2)

where E_{g1} and E_{g2} are the values of E_g for pure BN and the corresponding complexes, respectively. A standard method to specify the electrical conductance and its relation with the HOMO/LUMO gap energy (E_g) of semiconductor materials can be expressed as follows [35]:

$\sigma = AT^{3/2} \exp(-E_g/2kT)$ (3)

where A (electrons/$m^3K^{3/2}$) is a constant and k is the Boltzmann's constant. This manner is approximately consistent with the experimental results. The density of states (DOS) plots was analyzed using the GaussSum code [36].

3. RESULTS AND DISCUSSION

3.1. Optimized structural characteristics of pure BN-sheet

The optimized structure of the pure BN-sheet and its HOMO and LUMO maps are represented in Fig. 1. The B-N bond length is about 1.45 Å, which is confirmed by previous reports [37, 38]. The end edges of the BN-sheet are saturated with hydrogen atoms to inhibit the boundary effects. The HOMO and LUMO orbitals mostly concentrated on the N and B atoms, respectively, indicating electron-rich N atoms and electron deficient B atoms as adsorption sites in the BN-sheet. Due to the more different electronegativity between N and B atoms of the BN-sheet, possess negative and positive electrostatic potential, respectively, which exhibits the partial ionic nature of B-N bonds in the sheet. This is the basis of the wide applications of the BN nanostructures in the electronics and gas sensing. Also, natural bond orbitals (NBO) analysis indicated a positive charge value of about 1.4 e on the B atoms and negative charge with the same value on the N atoms in the central ring of the BN-sheet. The magnitude of dipole moment of the pure BN-sheet is about 0.13 Debye, and its computed energy gap (E_g) by about 7.91 eV which is highly larger than that of E_g of the graphene (0.32 eV) [38]. Therefore, in comparison with the semimetal behavior of graphene, the BN-sheet mostly exhibits a semiconductor property. Also, the density of states (DOS) analysis of pure sheet is displayed in Fig. 1.

3.2. Adsorption of $POCl_3$ on the pure BN-sheet

To earn the most stable complexes of $POCl_3$/BN, numerous achievable initial structures were studied with different modes and orientations near the BN sheet surface. The oxygen and chlorine atoms of $POCl_3$ molecule possess unlocalized lone pairs that can be interacted with the empty 2p orbitals of B atoms of the sheet; hence, these atoms are located on the B atoms of the sheet. Also, molecular potential electrostatic (MEP) map of $POCl_3$ molecule (Fig. 2) was explored to scrutinize the molecular adsorption

process. As seen in Fig. 2, the negative electrostatic potential on oxygen atom can interact with any positive site. After the structural optimization process, only one kind of the most stable configuration was obtained with minima potential energy. Table 1 summarizes the adsorption energy, net charge transfer, HOMO and LUMO energies, energy gap (E_g), and changes of E_g ($\%\Delta E_g$) for this structure.

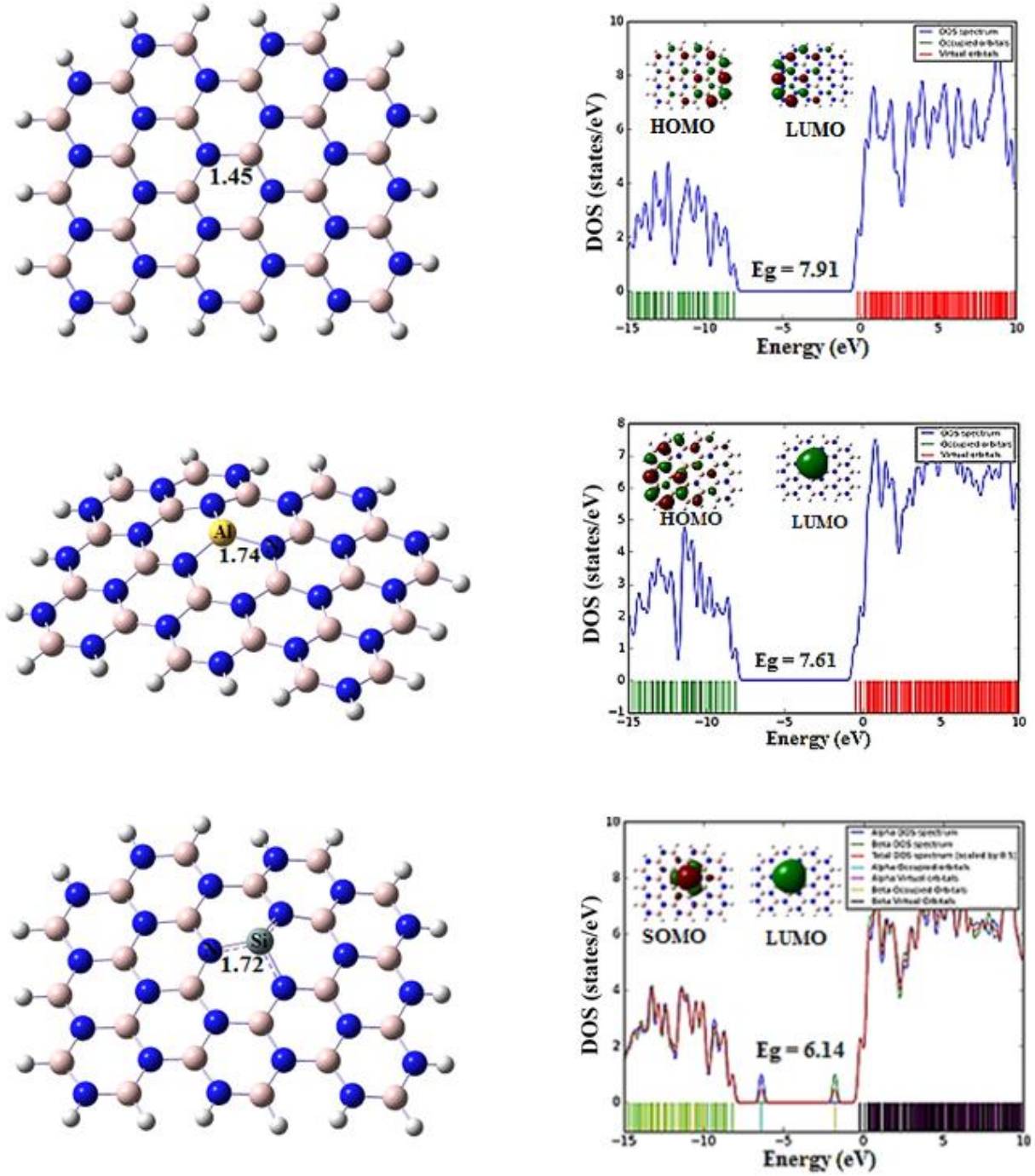

Fig. 1. Optimized structures and density of states (DOSs) plots of the pure, Al- and Si-doped BN sheet. The distances are in A°.

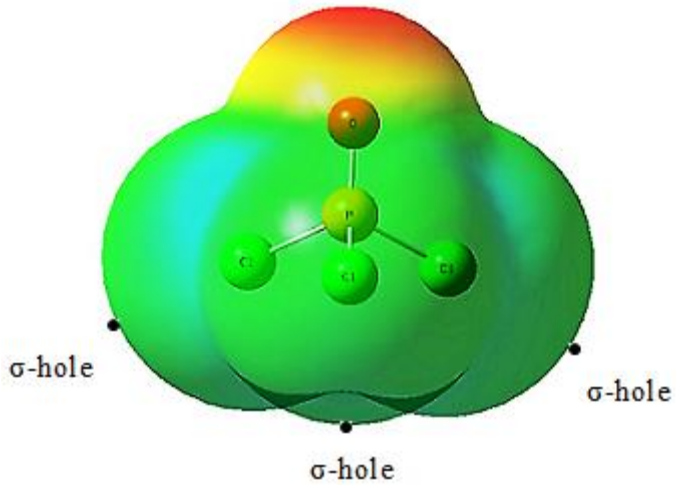

Fig. 2. Calculated molecular electrostatic potential (MEP) surface map of the $POCl_3$ molecule. Color ranges are in a.u.: -0.031 > red; -0.031 > yellow > 0; blue > 0.031.

Table 1. Calculated adsorption energies (E_{ad}, kcal mol^{-1}), charge transfer (Q_T, e), HOMO and LUMO energies (eV), HOMO-LUMO energy gap (E_g, eV), and change of the E_g ($\%\Delta E_g$) upon the adsorption of $POCl_3$ molecule

Structure	E_{ad} (kcal mol^{-1})	Q_T (e)	E_{HOMO} (eV)	E_{LUMO} (eV)	E_g (eV)	$\%\Delta E_g$
BN	-	-	-8.14	-0.23	7.91	-
A	-8.64	0.030	-8.12	-1.44	6.68	-15.55
Al-BN	-	-	-8.13	-0.52	7.61	-
B	-37.01	0.153	-7.79	-2.31	5.48	-27.99
Si-BN	-	-	-6.38	-0.24	6.14	-
C	-62.01	0.684	-7.55	-0.35	7.2	17.26

The orbitals between O atom of $POCl_3$ and B atom of sheet (O-B) overlap strongly in the most stable configuration (complex A), leading to the formation of a strong O-B bond with an interaction distance of about 2.83 Å. Upon the adsorption process, rehybridization of B atom, as the adsorption site from sp^2 to sp^3, results in local slight deformation of sheet. Also, the P-O bond length of $POCl_3$ molecule is expanded (1.46 Å) after the adsorption process compared to the free molecule in gas phase (1.45 Å), indicating a significant interaction between O atom and the sheet surface. The adsorption energy of this complex is reported by about -8.64 kcal mol^{-1}. Based on the NBO analysis, a charge transfer value of about 0.03 e is transferred from the molecule to the sheet being greater than other complexes, confirming the strong interaction. To examine further adsorption process effects of the target molecule on the sheet electronic properties, density of states (DOS) plots and HOMO and LUMO maps for the most stable complexes are shown in Fig. 3.

The adsorption of $POCl_3$ molecule on the sheet in the complex of $POCl_3$/BN sheet led to creation of new electronic states near the LUMO state and upper the HOMO state within the E_g. Changes of DOS complexes indicate high sensitivity of the sheet electronic properties to the adsorption of $POCl_3$ molecule. As seen in Table 1, both the HOMO and LUMO states are slightly stabilized to the lower energies, in which E_g value decreases from

7.91 eV in the bare sheet to 6.68 eV in the complex of $POCl_3$/BN (ΔE_g = 15.55%).

The electronic conductance changes decrease because of less band gap changes according to Eq. (3), which are converted to negligible weak electrical signals in electronic circuits. Thus, it can be concluded that the interaction between the molecule and BN-sheet alters the sheet electronic structure. However, the pure BN-sheet cannot be used as a proper sensor for detecting the molecule due to the weak adsorption energy and low adsorption capacity. Thus, there is a need to modify the structure to improve its elctronic sensitivity.

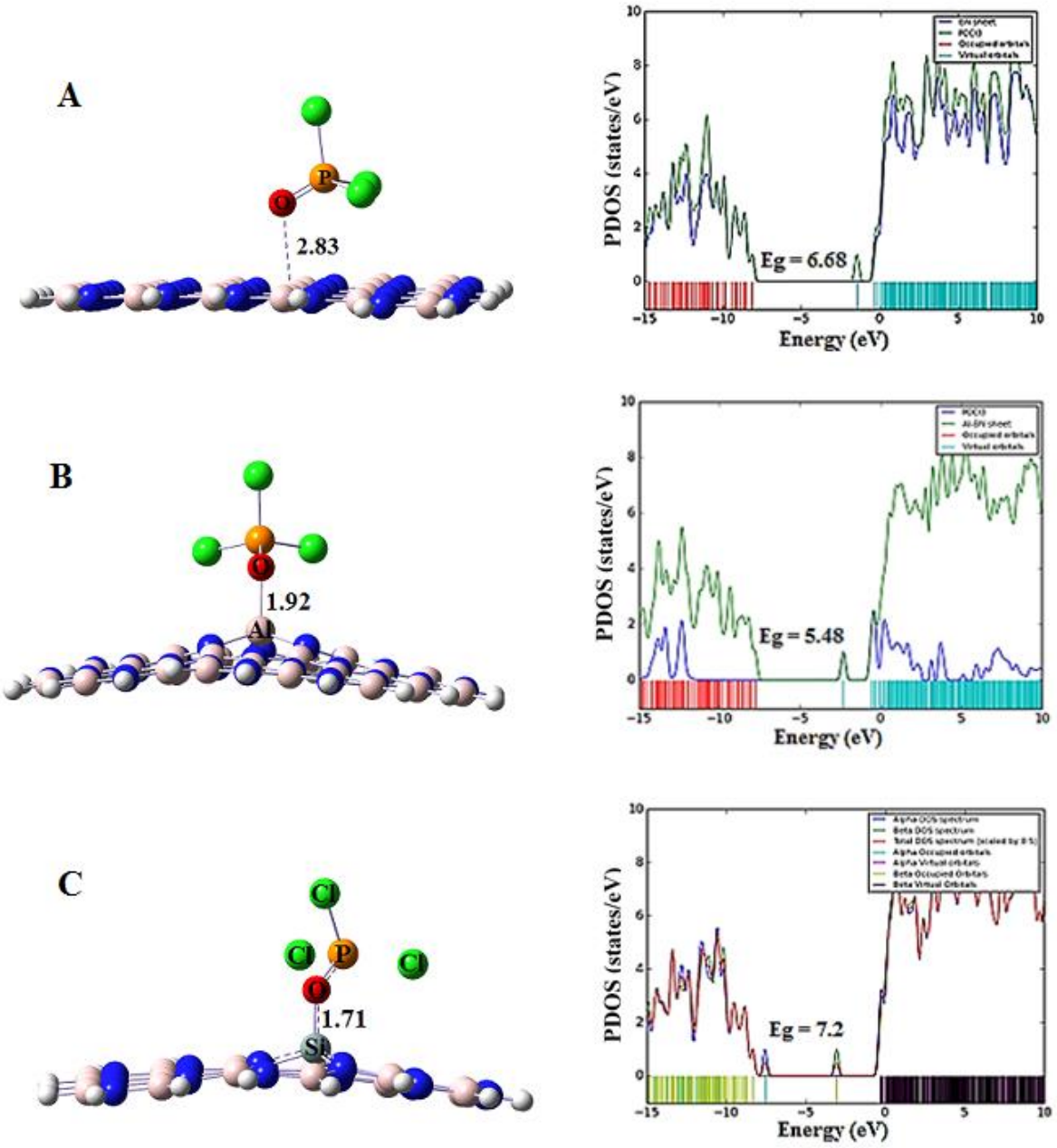

Fig. 3. Optimized structures of the most stable complexes of (A) $POCl_3$/BN, (B) $POCl_3$/Al-BN, and (C) $POCl_3$/Si-BN and corresponding partial density of states (PDOS) plots. The distances are in A°.

3.3. Modification of the BN sheet structure with Al-doping- and Si-doping

3.3.1. Adsorption of $POCl_3$ on Al-BN sheet

To achieve suitable chemical gas sensors with high performance, this study sought to modify the BN sheet structure to resolve this enigma because of the insensitivity of the pure BN-sheet to $POCl_3$ molecule. One of the ways to improve the electronic sensitivity of nanostructures is chemical doping process, which changes the electronic structure of the sheet. Many papers have reported that adding heteroatoms to nanomaterial structures could improve their reactivity and sensitivity to adsorbate molecules [39-43]. In the current work, a B atom of the BN-sheet as an active site is substituted by an Al atom, and the newly formed Al-N bond length (1.74 Å) is larger than the corresponding B-N bond length (1.45 Å) (Fig. 1). The calculations indicate that replacing N atom by Al atom is energetically unfavorable. Due to the larger size of Al atom than B atom, doped Al atom projected slightly out of the plane (Fig. 1) and its rehybridization from sp^2 to sp^3 cause slightly deformed structure of sheet near the doped site; besides, its electronic properties suffer great changes. After the encapsulation of Al atom in the sheet, E_g value decreased from 7.91 eV (bare BN-sheet) to 7.61 eV (Al-BN sheet) upon the optimization process, in which the LUMO state shifts from -0.23 eV to lower energies (-0.52 eV) and is stabilized slightly. The less changes of E_g indicate that B and Al atoms have valence isoelectronic, as a result, there are not much differences in the electronic properties between the BN-sheet and Al-BN sheet. Also, the estimated value of dipole moment is about 0.32 Debye for the Al-BN model. Based on the DOS plot of the Al-BN sheet (Fig. 1), the gap energy decreases slightly due to the appearance of new quantum state near the LUMO state. According to the molecular electrostatic potential (MEP) surface of Al-BN sheet (Fig. 4(a)), positive electrostatic region on Al atom can interact with each negative electrostatic site of adsorbate.

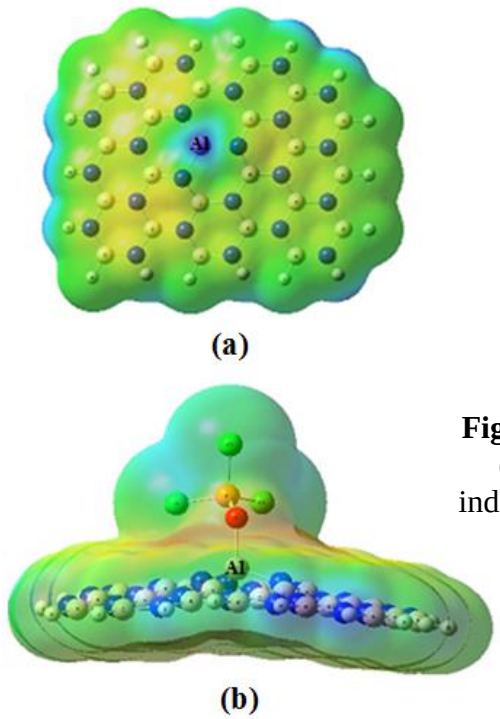

Fig. 4. The MEP of (a) Al-BN sheet and (b) the most stable complex ($POCl_3$/Al-BN sheet); blue color on Al atom indicates the positive electrostatic potential and red color on oxygen atom of the complex denotes the negative electrostatic potential.

In the most stable complex ($POCl_3$/Al-BN sheet), $POCl_3$ molecule is linked from posphoryl group (-P=O) oxygen atom to Al atom with a O-Al bond length of about 1.92 Å (Fig. 3) and an evaluated adsorption energy of about -37.01 kcal mol^{-1} being high greater than that of the pure sheet (Table 1). In this complex, oxygen atom with high nucleophilic nature tends to attach Al atom depletion electron, leading to the chemisorption (strong interaction) and a remarkable increase in the sheet reactivity. The chlorine atoms of $POCl_3$ molecule, however, interact somewhat weakly with the Al-BN than that of oxygen atom owing to the σ-holes (positive electrostatic potential regions) of chlorine halogens. To explore the electronic sensitivity of the Al-BN to $POCl_3$ molecule, drown density of states (DOS) plot of Al-BN is compared with the pure BN-sheet (Fig. 3). This comparison clearly illustrates significant difference of their DOS plots due to the stronger interaction of $POCl_3$ with the Al-BN. Upon the $POCl_3$ chemical adsorption process on the Al-BN, E_g value noticeably decreases from 7.61 (bare Al-BN) to 5.48 eV ($POCl_3$/Al-BN complex) and the sheet represents more semiconducting property. The HOMO state slightly shifts to upper energies (from -8.13 to -7.79 eV), and destabilized slightly, but the LUMO state is notably stabilized with shifting from -0.52 to -2.31 eV, leading to a dramatic decrease in E_g value (Table 1). Based on Eq. (3), the great changes in E_g result in major variations in the electrical conductivity of Al-BN, which demonstrate the high sensitivity of electronic properties of Al-BN to $POCl_3$ adsorption. Therefore, it can be concluded that the Al-BN is a suitable chemical sensor for detecting $POCl_3$ molecule. Based on our prediction, the adsorption of $POCl_3$ on the Al-BN sheet may be reversible because of the moderate E_{ad}. It is worth noting that very strong interactions are not favorable in gas detection because of hard desorption and subsequently a great recovery time. The recovery time of nanostructures can be reached through the transition state theory [44]:

$$\tau = \nu_0^{-1} \exp(-E_{ad}/kT) \quad (4)$$

where τ is recovery time, T is the temperature, k is Boltzmann's constant, and ν_0 is the attempt frequency. According to this equation, more negative E_{ad} values will enhance the recovery time in an exponential manner. However, the estimated E_{ad} of $POCl_3$ in the Al-BN system is not very large to disallow the recovery of the sensor, and the recovery time will be minor.

3.3.2. Adsorption of $POCl_3$ on Si-BN sheet

The basic decision in this paper is to probe the reliable gas sensors to detect $POCl_3$ molecule. Therefore, the effects of Si atom inclusion into the sheet was investigated here to determine the reactivity of the BN sheet to $POCl_3$ and its electronic properties. The optimized structure of Si-BN sheet is shown in Fig. 1. Numerous theoretical approaches based on the Si-doping have already investigated and reported their synthesis [45-48]. When a B atom of sheet is replaced by a Si atom, the geometry structural of the sheet is slightly distorted in the adjacency of doped Si site and doped Si atom is slightly pulled out of the sheet surface to reduce pressing. The newly made Si-N bond length of about 1.72 Å is greater than the B-N (BN sheet) and lesser than the Al-N (Al-BN) because of the lower radius of Si atom (~1.46 Å) than that of Al atom (~1.82 Å) and larger than that of B atom (~1.17 Å). The NBO analysis indicates that the hybridization of sp^3 for Si atom with a high coordination number is more accessible for interaction against adsorbates. The E_g of about 6.14 eV computed for Si-BN is lower than that

of pristine BN and Al-BN. The lower E_g value is attributed to the lower kinetic stability and higher reactivity of the sheet. Thus, the electronic property of Si-BN is considerably different from those of the other sheets. Owing to the electronegativity difference between Si and N atoms of the sheet, the charge transfer from Si to B atom causes a positive charge of about 3.19 e on the Si atom and average negative charges in the range of -1.79 to -1.97 e on the neighboring N atoms, based on the natural population analysis (NPA). Also, spin density surface analysis (Fig. 5) exhibits that high spin density accumulation on the Si atom helps the BN sheet to be more active by dopant Si.

The Si-BN structure possesses a dipole moment of 0.59 Debye magnitude. The HOMO-LUMO orbitals of Si-BN are noticeably different from those of the other BNNs. The HOMO state of the Si-BN is singly occupied by electron molecular orbital (SOMO) that tends to donate electron to the electrophilic groups, and is located on the doped Si atom. The energy of SOMO state of Si-BN is greater by about 0.89 eV than the HOMO state of pristine BN, making it more accessible for electrophilic attacks. On the other hand, the LUMO state is centralized on the Si atom, which can also have the role of the acceptor electron, and this adsorption site is suitable for nucleophilic attacks. Upon the adsorption of $POCl_3$ molecule on the Si-BN, our calculations indicate that $POCl_3$ molecule mostly tends to interact with Si atom of the sheet from phosphoryl group (-P=O) oxygen side in the most stable complex. The equilibrium interaction distance and the corresponding adsorption energy are about 1.71 Å and -62.01 kcal mol^{-1}, respectively. The much greater adsorption energy indicates the stronger interaction of $POCl_3$ with Si-BN than with Al-BN. As mentioned previously, a great adsorption energy is not favorable to sensing devices due to the hard recovery of sensor and increments in the molecule desorption time, which account for the disadvantages of these sensors. However, the potential application of Si-BN is dissociation of the poisonous $POCl_3$ gas in the environment (regarding the kind mode or orientation of gas molecule) to less toxic fragments and removing its toxicity effects. The local curvature and rehybridization of doped Si of the sheet structure Likely lead to the enhanced reactivity of the nanosheet. Upon the adsorption process, the electronic properties of sheet also changed sensibly. Table 1 and DOS analysis (Fig. 3C) clearly indicate that the E_g value increases by about ~17.26% from 6.14 (bare Si-BN) to 7.20 eV ($POCl_3$/Si-BN complex). It can, therefore, be concluded that the electronic structure of the sheet is significantly affected upon the $POCl_3$ adsorption. Based

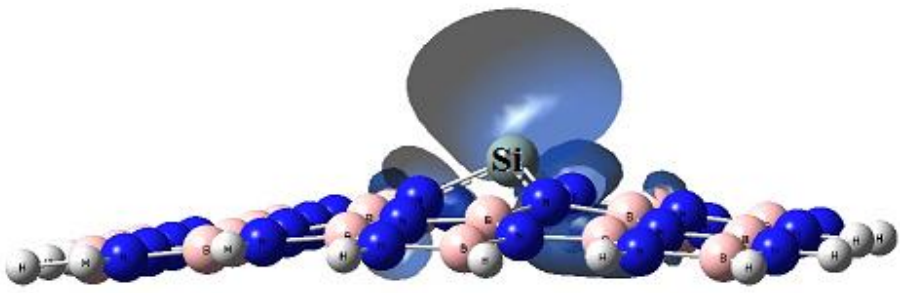

Fig. 5. The spin density surface (SDS) profile of Si-BN sheet indicating high spin density accumulation over Si-doped atom.

on Eq. (3), this results in more variations in the electrical conductivity of the material that can be converted to an electrical signal to diagnose $POCl_3$ molecule. According to Eq. (4), however, it cannot be utilized as an efficient sensor to detect this molecule because of the great adsorption energy and large recovery time.

3.3.3. Response and selectivity of the nanosensor

According to our calculations, since the Al-BN sheet is recognized as a good sensor for detecting $POCl_3$ gas, the effects of the disturbing air gases, such as O_2, N_2, and CO_2, were explored on the sensor selectivity. These gases were adsorbed on Al-BN sheet and computations were performed on the same level of theory. The adsorption energy of CO_2 gas is the highest value among small nonpolar molecules (O_2, N_2) due to the high molecular mass, size, and polarizability effects. CO_2 gas tends to interact with doped Al atom of the sheet through the oxygen atom with an adsorption energy of about -11.24 kcal mol^{-1} and an equilibrium distance of about 2.10 Å. The numerical results of E_{ad} and the electronic properties (Table 2), as well as large interaction distances (Fig. 6) suggest that the interactions of these gases with Al-BN are very weaker than with $POCl_3$ gas.

These weak interactions are attributed to the appearance of instantaneous dipole moment and induced dipole moment on the sheet structure and nonpolar molecules (Van der Waals forces). The electronic structure of the sensor could not be affected by weak interactions (lower adsorption energy values), as a result, the sensor can detect $POCl_3$ gas in the presence of the other disturbing gases. It can be suggested that Al-BN possess a high selectivity to identify the probe molecule.

4. CONCLUSION

The electronic properties and surface reactivity of BN nanosheets were explored through DFT calculations. The results indicate that Al-doping is an effective method to improve the electronic sensitivities of BN and Al-BN. Hence, it could be utilized as a potential material to recognize $POCl_3$ molecule as it possesses high selectivity even in the presence of air disturbing gases. Si-doping inside the BN, on the other hand, causes a higher reactivity of Si-BN due to the chemisorption of molecule, in which the doped Si creates a catalytic active site on the sheet surface, leading to remarkable changes of the electronic properties. Owing to the higher adsorption energy and larger recovery time, however, the sensor does not function well for a toxic gas. Our results present deeper insight about the properties of BN nanostructures and the effects of adsorbed molecules on their electronic properties, which help to develop gas sensors with fast response and high sensitivity in nanodevices.

Table 2. The adsorption energies (E_{ad}), HOMO and LUMO energies, HOMO/LUMO gap (E_g), and the change energy upon the adsorption of air gases (N_2, O_2, and CO_2) on Al-BN sheet

Configurations	E_{ad} (kcal mol^{-1})	E_{HOMO} (eV)	E_{LUMO} (eV)	E_g (eV)	$\%\Delta E_g$
N_2-Al-BN	-3.78	-8.12	-0.54	7.58	-0.39
O_2-Al-BN	-4.73	-8.07	-0.22	7.85	3.15
CO_2-Al-BN	-11.24	-7.97	-0.70	7.27	-4.46

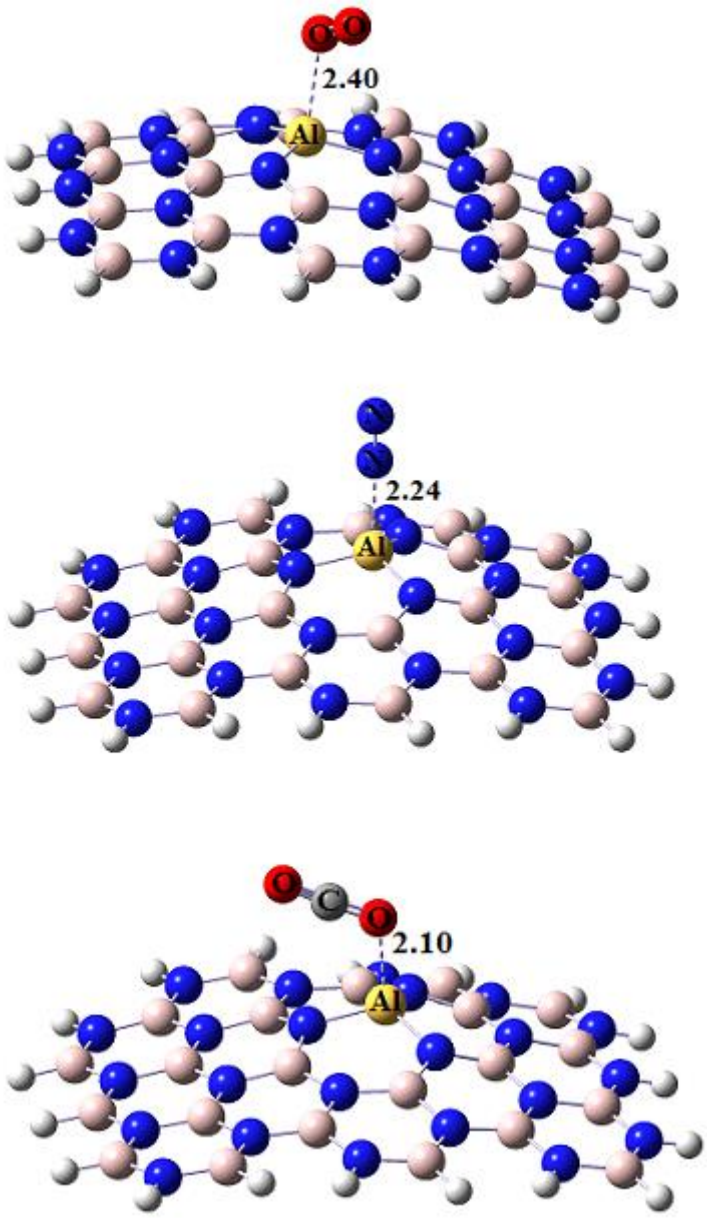

Fig. 6. The optimized most stable configurations of O_2, N_2, and CO_2 gases on Al-BN sheet. The distances are in Å.

REFERENCES

[1] A. D. F. Toy, The Chemistry of Phosphorus. Pergamon Press, Oxford, UK. 1973.

[2] W. Yim, X.G. Gong, Z. Liu, Chemisorption of NO_2 on carbon nanotubes, Journal of Physical Chemistry B. 107 (2003) 9363–9369.

[3] Z. Bagheri, A. A. Peyghan, DFT study of NO□2 adsorption on the AlN nanocones, Comput. Theor. Chem. 1008 (2013) 20–26.

[4] J. Beheshtian, A. A. Peyghan, Z. Bagheri, Sensing behavior of Al-rich AlN nanotube toward hydrogen cyanide, J. Mol. Model. 19 (2013) 2197–2203.

[5] Y. Valadbeigi, H. Farrokhpour, M. Tabrizchi, Adsorption of small gas molecules on B36 nanocluster, Journal of

Chemical Sciences. 127 (2015) 2029-2038.

[6] T. Liu, Y. Chen, M. Zhang, L. Yuan, C. Zhang, J. Wang, J. Fan, A first-principles study of gas molecule adsorption on borophene, Aip Advances. 7 (2017) 125007.

[7] C. S. Huang, A. Murat, V. Babar, E. Montes, U. Schwingenschlögl, Adsorption of the Gas Molecules NH_3, NO, NO_2, and CO on Borophene. The Journal of Physical Chemistry C. 122 (2018) 14665-14670.

[8] R. Freitas, G. K. Gueorguiev, F. de Brito Mota, C. de Castilho, S. Stafström, A. Kakanakova-Georgieva, Reactivity of adducts relevant to the deposition of hexagonal BN from first-principles calculations, Chem. Phys. Lett. 583 (2013) 119–124.

[9] E. Salih, M. Mekawy, R. Y. A. Hassan, I. M. El-Sherbiny, Synthesis, characterization and electrochemical-sensor applications of zinc oxide/graphene oxide nanocomposite, J. Nanostruct. Chem. 6 (2016) 137–144.

[10] C.-W. Lin, K.-L. Huang, K.-W. Chang, J.-H. Chen, K.-L. Chen, C.-H. Wu, Ultraviolet photodetector and gas sensor based on amorphous In-Ga-Zn-O film, Thin Solid Films. 618 (2016) 73–76.

[11] A. M. Attaran, S. Abdol-Manafi, M. Javanbakht, M. Enhessari, Voltammetric sensor based on Co_3O_4/SnO_2 nanopowders for determination of diltiazem in tablets and biological fluids, J. Nanostruct. Chem. 6 (2016) 121–128.

[12] [12] M. Eslami, V. Vahabi, A. A. Peyghan, Sensing properties of BN nanotube toward carcinogenic 4-chloroaniline: a computational study, Phys. E. 76 (2016) 6–11.

[13] R. Yakimova, A. Kakanakova-Georgieva, G. R. Yazdi, G. K. Gueorguiev, M. Syväjärvi, Sublimation growth of AlN crystals: growth mode and structure evolution, J. Cryst. Growth. 281 (2005) 81–86.

[14] A. A. Peyghan, M. T. Baei, M. Moghimi, S. Hashemian, Adsorption and electronic structure study of imidazole on (6, 0) zigzag single-walled boron nitride nanotube, J. Clust. Sci. 24 (2012) 31–47.

[15] A. A. Peyghan, M. Noei, Electronic response of nano-sized cages of ZnO and MgO to presence of nitric oxide, Chin. J. Chem. Phys. 26 (2013) 231–236.

[16] D. Robati, S. Bagheriyan, M. Rajabi, O. Moradi, A. A. Peyghan, Effect of electrostatic interaction on the methylene blue and methyl orange adsorption by the pristine and functionalized carbon nanotubes, Physica E: Low-Dimens. Syst. Nanostruct. 83 (2016) 1–6.

[17] A. A. Peyghan, S. F. Rastegar, Z. Bagheri, Selective detection of F2 in the presence of CO, N_2, O_2, and H_2 molecules using a ZnO nanocluster, Mon. Chem.-Chem. Mon. 146 (2015) 1233–1239.

[18] A. A. Peyghan, H. Soleymanabadi, Z. Bagheri, Theoretical study of carbonyl sulfide adsorption on Ag-doped SiC nanotubes, J. Iran. Chem. Soc. 12 (2015) 1071–1076.

[19] A. Ahmadi, N. L. Hadipour, M. Kamfiroozi, Z. Bagheri, Theoretical study of aluminum nitride nanotubes for chemical sensing of formaldehyde, Sens, Actuators B: Chem. 161 (2012) 1025–1029.

[20] A. Ahmadi Peyghan, N. L. Hadipour, Z. Bagheri, Effects of Al doping and doubleantisite defect on the adsorption of HCN on a BC2N nanotube: density functional theory studies, J. Phys. Chem. C. 117 (2013) 2427–2432.

[21] J. Beheshtian, A. A. Peyghan, Z. Bagheri, Detection of phosgene by Sc-doped BN nanotubes: a DFT study, Sens. Actuators B: Chem. (2012) 846–852.

[22] J. Beheshtian, A. A. Peyghan, Z. Bagheri, Carbon nanotube functionalization with carboxylic derivatives: a DFT study, J. Mol. Model. 19 (2012) 391-396.

[23] Q. Cao, J. A. Rogers, Ultrathin films of single-walled carbon nanotubes for

electronics and sensors: a review of fundamental and applied aspects, Advanced Materials. 21 (2009) 29-53.
[24] J. Beheshtian, A. Ahmadi Peyghan, Z. Bagheri, Hydrogen dissociation on diene functionalized carbon nanotubes, J. Mol. Model. 19 (2012) 255-261.
[25] S. H. Lim, J. Luo, W. Ji, J. Lin, Synthesis of boron nitride nanotubes and its hydrogen uptake, Catalysis Today. 120 (2007) 346–350.
[26] C. Li, Y. Bando, C.Y. Zhi, Y. Huang, D. Golberg, Thickness-dependent bending modulus of hexagonal boron nitride nanosheets, Nanotechnology. 20 (2009) 385707.
[27] H. M. Ghassemi, C.H. Lee, Y.K. Yap, R. S. Yassar, In situ TEM monitoring of thermal decomposition in individual boron nitride nanotubes, JOM. 62 (2010) 69.
[28] Y. H. Zhang, K. G. Zhou, X. C Gou, et al, Effects of dopant and defect on the adsorption of carbon monoxide on graphitic boron nitride sheet: a first-principles study, Chem. Phys. Lett. 484 (2010) 266–270.
[29] Y. Q. Zhang, Y. J. Liu, , Y. L. Liu, J. X. Zhao, Boosting sensitivity of boron nitride nanotube (BNNT) to nitrogen dioxide by Fe encapsulation, Journal of Molecular Graphics and Modelling. 51 (2014) 1-6.
[30] R. Wang, R. Zhu, D. Zhang, Adsorption of formaldehyde molecule on the pristine and silicon-doped boron nitride nanotubes, Chem. Phys. Lett. 467 (2008) 131–135.
[31] Y. J. Cho, C. H. Kim, H. S. Kim, J. Park, H. C. Choi, H. J. Shin, G. H. Gao, H. S. Kang, Electronic Structure of Si-Doped BN Nanotubes Using X-ray Photoelectron Spectroscopy and First-Principles Calculation, Chem. Mater. 21 (2009) 136.
[32] M. Frisch, G. Trucks, H. B. Schlegel, G. Scuseria, M. Robb, J. Cheeseman, G. Scalmani, V. Barone, B. Mennucci, G. Petersson, Gaussian 09, Revision B.01, Gaussian, Inc. Wallingford. CT. 200 (2009).
[33] Y. Zhao, N. E. Schultz, D. G. Truhlar, Exchange-correlation functional with broad accuracy for metallic and nonmetallic compounds, kinetics, and noncovalent interactions, J. Chem. Phys. 123 (2005) 161103.
[34] S. F. Boys, F. d. Bernardi, The calculation of small molecular interactions by the differences of separate total energies. Some procedures with reduced errors, Mol. Phys. 19 (1970) 553.
[35] A. Ahmadi Peyghan, N. Hadipour, Z. Bagheri, Effects of Al-Doping and double-Antisite defect on the adsorption of HCN on a BC2N nanotube: DFT studies, J. Phys. Chem. C. 117 (2013) 2427–2432.
[36] N. M. O'boyle, A. L. Tenderholt, K. M. Langner, Cclib: a library 446 for package-independent computational chemistry algorithms, J 447 Comput Chem. 29 (2008) 839–845.
[37] M. Samadizadeh, A. A. Peyghan, S. F. Rastegar, Sensing behavior of BN nanosheet toward nitrous oxide: A DFT study, Chinese Chemical Letters. 26 (2015) 1042-1045.
[38] A. A. Peyghan, M. Noei, S. Yourdkhani, Al-doped graphene-like BN nanosheet as a sensor for para-nitrophenol: DFT study, Superlattices Microstruct. 59 (2013) 115–122.
[39] E. Shakerzadeh, E. Khodayar, S. Noorizadeh, Theoretical assessment of phosgene adsorption behavior onto pristine, Al- and Ga-doped B12N12 and B16N16 nanoclusters, Comput. Mater. Sci. 118 (2016) 155–171.
[40] J. Beheshtian, A.A. Peyghan, M. Noei, Sensing behavior of Al and Si doped BC3 graphenes to formaldehyde, Sens. Actuators B: Chem. 181 (2013) 829–834.
[41] M. T. Baei, A. A. Peyghan, Z. Bagheri, M. B. Tabar, B-doping makes the carbon nanocones sensitive towards NO molecules, Physics Letters A. 377 (2012) 107–111.
[42] Y. C. Kim, C. H. Yoon, J. Park, J. Yoon, N. S. Han, J. K. Song, S. M. Park, J. S.

Ha, Effect of Sb doping on the opto-electronic properties of SnO_2 nanowires, Thin Solid Films. 520 (2012) 6471-6475.
[43] A. A. Peyghan, M. Noei, M. B. Tabar, A large gap opening of graphene induced by the adsorption of Co on the Al-doped site, Journal of molecular modeling. 19 (2013) 3007-3014.
[44] A. A. Peyghan, A. Soltani, A. A. Pahlevani, Y. Kanani, S. Khajeh, A first-principles study of the adsorption behavior of CO on Al-and Ga-doped single-walled BN nanotubes, Applied Surface Science. 270 (2013) 25-32.
[45] J. Li, Y. Lu, Q. Ye, M. Cinke, J. Han, M. Meyyappan, Carbon nanotube sensors for gas and organic vapor detection, Nano Letters. 3 (2003) 929–933.
[46] J. Beheshtian, A. A. Peyghan, Z. Bagheri, Detection of phosgene by Sc-doped BN nanotubes: a DFT study, Sens. Actuators B Chem. 846 (2012) 852.
[47] S. Sharma, A. S. Verma, A theoretical study of H_2S adsorption on grapheme doped with B, Al and Ga, Phys. B. 427 (2013) 12-16.
[48] R. Wang, R. Zhu, D. Zhang, Adsorption of formaldehyde molecule on the pristine and silicon-doped boron nitride nanotubes, Chem. Phys. Lett. 467 (2008) 131–135.

مجله شیمی فیزیک و شیمی نظری
دانشگاه آزاد اسلامی واحد علوم و تحقیقات
جلد ۱۶، شماره ۳ و۴، پاییز و زمستان ۱۳۹۸
ISSN ۱۷۳۵-۲۱۲۶

مطالعه نظری ادوات نانوحسگری بر پایه نانوورقه بور نیتریدی برای شناسایی مولکول POCl3

رقیه مولادوست*

دانشگاه محقق اردبیلی، دانشکده علوم پایه، گروه شیمی، اردبیل، ایران

چکیده

فرآیند جذب سطحی مولکول POCl3 بر روی سطوح نانوورقه‌های BN ، Al-BN و Si-BN به‌منظور شناسایی آن با رهیافت تئوری تابعی چگالی (DFT) مورد بررسی قرار گرفت. پایدارترین کمپلکس‌های جذب شامل POCl3/BN (O-B)، POCl3/Al-BN (O-Al) و POCl3/Si-BN (O-Si) با انرژی‌های جذب ۸/٦٤- ، ۳۷/۰۱- و ٦۲/۰۱- کیلو کالری بر مول پیش‌بینی شدند. بعد از فرآیند جذب، پارامترهای محاسباتی نشان داد که برهمکنش Si-BN با مولکول POCl3 از لحاظ انرژیکی بسیار قوی می‌باشد که نشان‌دهنده واکنش‌پذیری بالای Si-BN با مولکول POCl3 است که منجر به تفکیک این مولکول سمی به اجزائی با اثر سمیت کمتر می‌شوند که برای حفاظت محیط‌زیست مضرات کمتری دارد. لازم به ذکر است که برهمکنش‌های خیلی قوی به دلیل زمان بازیابی بیشتر سنسور و واجذب سخت مولکول برای کارآمد بودن یک سنسور گازی مطلوب نمی‌باشد. نتایج مطالعات با آنالیز چگالی حالات الکترونی (DOS) نشان می‌دهد که در فرآیند جذب مولکول، حساسیت الکترونیکی Al-BN به مولکول POCl3 افزایش می‌یابد به‌طوری‌که دستخوش تغییر محسوسی در گپ انرژی HOMO/LUMO در حدود ۲۷/۹۹-٪ می‌شود. به‌طوری‌که مقدار بار الکترونی بزرگتری (QT) از مولکول POCl3 به سطح نانوورقه انتقال می‌یابد و حالات الکترونی جدیدی در محدوده باندگپ (Eg) ظاهر می‌شوند. در نتیجه، تغییرات در هدایت الکتریکی نانوورقه منجر به تولید سیگنال الکترونی در مدار الکتریکی برای شناسایی مولکول در محیط می‌شود. بنابراین، از Al-BN می‌توان به عنوان سنسور کارآمد برای شناسایی مولکول POCl3 استفاده نمود.

کلید واژه‌ها: نانوورقه بور نیتریدی، تئوری تابعی چگالی، فسفریل کلرید، خواص حسگری

* مسئول مکاتبات: moladoust_100@yahoo.com